ELSEVIER

Journal of Nuclear Materials 258–263 (1998) 858–864

journal of nuclear materials

Experiments with tungsten limiters in TEXTOR-94

V. Philipps [a,*], A. Pospieszczyk [a], A. Huber [a], A. Kirschner [a], J. Rapp [a], B. Schweer [a], P. Wienhold [a], G. van Oost [b], G. Sergienko [c], T. Tanabe [d], K. Ohya [e], M. Wada [f], T. Ohgo [g], M. Rubel [h]

[a] *Institut für Plasmaphysik, Forschungszentrum Jülich, Euratom Association-KFA, D-52425 Jülich, Germany* [1]
[b] *Laboratoire des Plasma, Laboratorium voor Plasmafysica, Association Euratom Belgian State, Brussels, Belgium*[1]
[c] *Institute for High Temperatures of the RAS, Ass. IVTAN, Rußland, Germany*
[d] *Nagoya University, Nagoya, Japan*
[e] *University of Tokushima, Tokushima, Japan*
[f] *Doshisha University, Kyoto, Japan*
[g] *Department of Physics, Fukuoka University of Education, Fukuoka, Japan*
[h] *Royal Institute of Technology, Physics Department Frascati, Association Euratom/NFR, Frescativagen, Sweden*

Abstract

The release of tungsten and light impurities from tungsten limiters exposed into the plasma edge of TEXTOR-94 has been measured by spectroscopic methods. Absolute effective tungsten sputtering yields are compared with model calculations on physical sputtering. The agreement is reasonable: however the observed strong decrease of tungsten release with increasing density cannot be fully explained. Erosion areas are clearly separated from carbon deposition zones. Surface analysis found neither carbon nor deuterium on the shiny metallic areas: A very sharp transition from ''clean'' metallic areas to carbon deposition zones within about 2–4 mm is found, instead. The carbon deposit is about 200–300 nm thick and contains deuterium with a D/C ratio of 0.05–0.1.

1. Introduction

Low Z materials like graphite, boron and beryllium have proven to be excellent plasma facing materials. Their main disadvantages are their large erosion rates by hydrogenic impact which may lead to reduced lifetimes under steady state operation conditions. Large erosion rates may also lead to large tritium inventories since the eroded material will be redeposited somewhere forming amorphous like layers, which can store large amounts of tritium by codeposition [1].

These are the main reasons to use high Z materials in fusion reactors. Their erosion by hydrogen impact is low with sputter threshold energies for deuterium and tritium impact as high as 80 and 60 eV, respectively, and their storage of tritium is expected to be low.

However, the high Z impurities in the plasma core lead to strong radiation losses, cooling of the plasma core and a reduced fusion rate. Moreover, high Z impurity transport may lead to impurity accumulation in the plasma center which is not tolerable for a fusion reactor. Thus the benefit of low or negligible impurity production at particle impact energies near the sputter threshold competes with the severe problem of strong radiation if suppression of impurity production is not sufficient or a small amount of released impurities accumulates in the plasma core.

Different studies with high Z wall materials in fusion devices have been started recently [2]. In ASDEX-U two full toroidal segments of the divertor strike zones have been replaced by tungsten coated graphite tiles [3]. The tungsten release from the plates decreased to negligible values under high density conditions under which where the plasma temperatures in front of the tiles decreased to values below 15 eV. Tungsten accumulation has been observed only in few cases which was accompanied with the disappearance of sawtooth activity. A full

* Corresponding author. Tel.: +49 2461 616331; fax: +49 2461 612660; e-mail: V.philipps@kfa-juelich.de.

[1] Partner in the Trilateral Euregio Cluster.

0022-3115/98/$19.00
PII: S0022-3115(98)00385-7

molybdenum inner wall and divertor tiles are used for longer times in ALCATOR-C mod [4].

In the tokamak TEXTOR-94 a high Z research program is performed since 1992 in the framework of the TEXTOR-IEA cooperation [5–7]. Accumulation of molybdenum and tungsten has regularly been observed under special conditions. The conditions for accumulation have been analyzed in TEXTOR in detail [8,9].

This contribution deals in particular with the tungsten release from and with deposition processes on a tungsten test limiter.

2. Experimental setup

TEXTOR-94 is limiter tokamak with a circular plasma of a minor radius of 46 cm and major radius of 175 cm. The plasma is limited at $r = 46$ cm by a toroidal graphite belt pump limiter with an area of 3.5 m^2. The wall temperature is normally kept at 600 K and boronization is applied about every 500–1000 shots. Additional heating can be provided by two neutral beam injectors (NBI) injecting tangentially in either the co or counter direction with a power of each up to 2 MW and/or by ICRH ion heating with a maximum power of about 6 MW.

Movable W-limiters with dimensions of 12 cm × 8 cm and a spherical shape with a radius of 7 cm were inserted through a limiter lock to the position of the LCFS or even deeper inside the minor plasma radius determined by the ALT-II limiter ($r = 46$ cm). The limiters were preheated to about 750 K from the rear by a resistively heated Mo-plate. Local limiter diagnostics is done using IR-thermography, calorimetry and visible spectroscopy. Spectroscopy included a tangential view with a spectrometer and 2D-CDD camera coupled to interference filters as well as a view from the top using another CCD-camera with interference filters. A schematic view of the experimental setup is shown in Fig. 1. From the spectra the temporal evolution of the intensities for different emission lines was evaluated using an image processor. The spectroscopic measurements provided spectra of intensities resolved in the minor radius at a fixed toroidal position (chosen near the locations of largest power loading) and integrated along the line of sight in poloidal direction. Edge electron temperature and density profiles were measured by means of atomic beam techniques (He and Li beams). The beams of deposited carbon and stored deuterium was measured post mortem by means of nuclear reaction analysis.

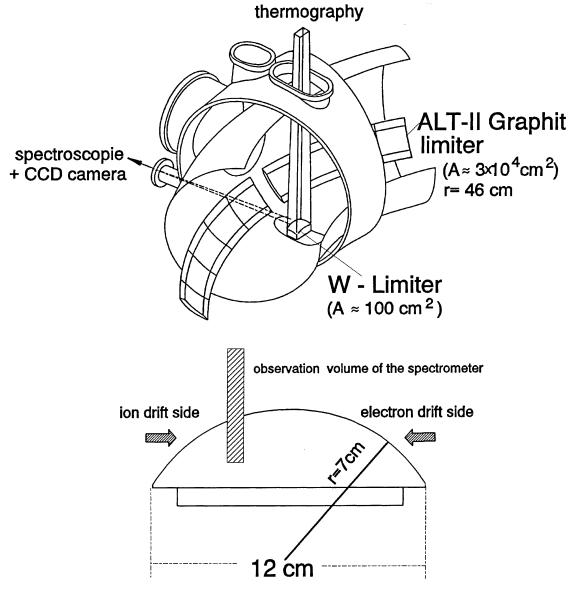

Fig. 1. Schematic view of the experimental setup. The limiters have toroidal and poloidal dimensions of 12 × 6 cm respectively and a spherical curvature with a radius of 7 cm.

3. Results and discussion

3.1. Tungsten impurity release

Tungsten test limiters have been positioned in TEXTOR typically at the radius of the ALT-II pump limiter ($r = 46$ cm) or 1–2 cm inside. Plasma temperatures at this radial position extend typically from about 30 up to 100 eV depending on heating scenario and plasma density. Fig. 2(a) and (b) show examples of the evolution of the line averaged density together with edge temperature and density at $r = 45$ cm for a plasma which was heated by NBI-co between 1–4.5 s and for which the density was raised during the NBI-heating phase. The plasma edge temperatures are comparably high causing significant W-release by physical sputtering. This sputtering is caused by hydrogenic impact and even more by carbon and oxygen impurity fluxes in the plasma boundary. Fig. 2(c) shows the relative carbon and oxygen fluxes emitted from the W-limiter for this discharge. Absolute carbon and oxygen flux ratios are obtained from Hα, Hγ, CII (267.7 and 657.8 nm) and the OII light (440 nm). Routinely the C/H flux ratio is evaluated from the CII-line at 426.7 nm and Hγ using a ratio of the ionization to photon rate (S/XB(CII): S/XB(Hγ)) of 28, which agreed well with the ratio evaluated from CII at 657 nm and Hα using S/XB values as described in the literature (see e.g. [10]). The O/H flux ratio is evaluated using a ratio S/XB (OII) to S/XB (Hγ) of 10. For the conditions shown in Fig. 2(a) the carbon and oxygen flux ratio is between 2% and 3%, not much dependent on the plasma density and heating scenario.

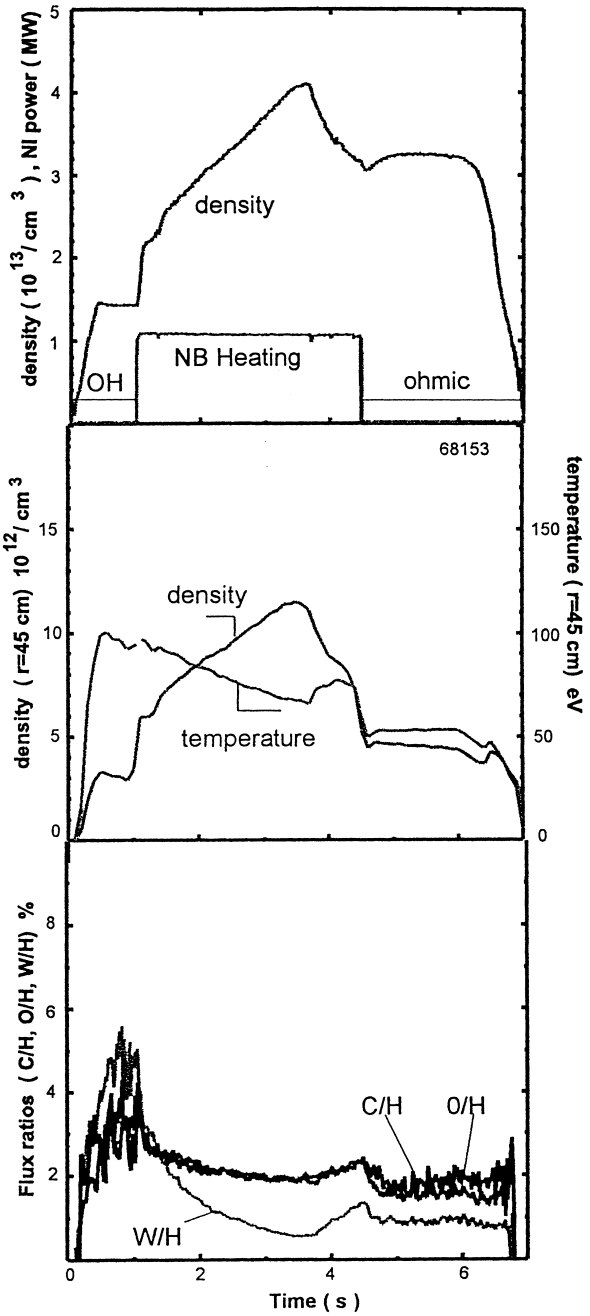

Fig. 2. Evolution of a discharge with an ohmic and hydrogen NI-co heated phase. W-limiter at $r = 45$ cm. (a) evolution of the line averaged density and NI-co heating; (b) evolution of density and temperature measured at $r = 45$ cm at the midplane; (c) evolution of the carbon, oxygen and tungsten flux ratio measured by spectroscopy.

This carbon flux ratio represents a typical value in TEXTOR at this radial position whereas the oxygen flux ratio varies depending on the wall conditioning situation. Fig. 2(c) shows also the flux ratio of W/H evaluated from a neutral WI line emission observed at 400.8 nm. The ionization events/ photon emission of this line has been measured recently [11] to about 30 in the temperature range of interest and a ratio of S/XB(WI) to S/XB(Hγ) of 0.03 has been used here. As can be seen, the W/H flux ratio decreases rather strongly with plasma density and decreasing edge electron temperature. Fig. 3 shows the density dependence of W/D effective emission yield for a larger set of shots measured during different campaigns. The data include ohmic and hydrogen NI-co heated plasmas with the limiter 1 cm inside the ALT limiter with a heating level of about 1–1.2 MW, as well as few shots at high densities (marked inside the square) where the external heating was raised from a level of 1 MW deuterium NI-co by addition of ICRH up to about 3 MW. As can be seen all these data fit rather well to the general trend of strongly decreasing effective W-emission rates with growing density. Addition of ICRH causes no unexpected W-release. The W-emission behavior shown in Fig. 2(c) has been modeled using the measured fluxes of carbon and oxygen (Fig. 2(c)), the edge temperature (Fig. 2(b)) and data on W-sputtering by deuterium, carbon and oxygen impact. Impact energies for deuterium carbon an oxygen are used according to $E_d = 5kT_e$ and $E_{c,o} = (2 + 3Z)kT_e$ assuming an impurity charge state of $Z = 4$ for carbon and oxygen (Fig. 4). A mixture of 50:50 for hydrogen to deuterium has been assumed as measured typically during hydrogen NBI heating of deuterium fueled plasmas. The figure shows that the agreement between the calculated effective W-sputtering yield and those measured spectroscopically is very good. A detailed comparison shows that measured W-release is stronger compared to the one in the ohmic start phase, where the plasma density is low (1.5×10^{13}/cm^3) and the edge temperature is as high as 100 eV. The decay of the measured W-influx during the NI heated phase with increasing plasma density is stronger and a fair agreement is obtained for the ohmic end phase where the plasma density is high and the temperature is low. Such a strong decay of W-release with decreasing edge temperature compared with calculations has already been observed in earlier experiments with tungsten test limiters [7]. The reason for this is not fully clear but might be due to a decreasing Ti/Te ratio with increasing density and under ohmic and NBI conditions at different density. An increase of density will also reduce the mean charge state of the light impurities, but this has been modeled with the TEXTOR-RITM code [12] and is not very important. One might also argue that incorporation of carbon in the tungsten surface by carbon impurity impact might alter the tungsten surface concentration and reduce sputtering at higher plasma densities. However, this seems unlikely due to experimental observations presented in the following section.

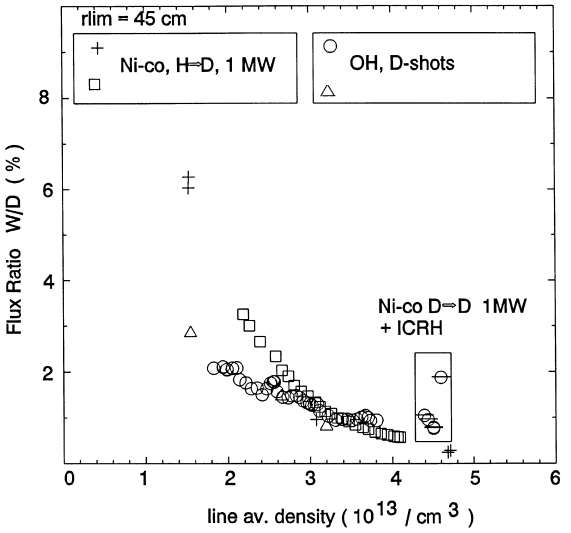

Fig. 3. Density dependence of the effective tungsten flux ratio W/D emitted from the W limiter. Data include ohmic, hydrogen heated NI-co and deuterium heated NI-co + ICRH heating (details in the figure) with the limiter at $r = 45$ cm.

3.2. Erosion and redeposition

3.2.1. Tungsten redeposition

The WI-line emission is a measure for gross-release of W atoms from the surface. The gross tungsten release, however, does not determine alone the net erosion or the plasma impurity contamination since a significant fraction of eroded tungsten is promptly ionized and redeposited back on the limiter surface, which greatly reduces the gross erosion and the plasma impurity contamination. As has been shown, enhanced redeposition will occur for sputtered tungsten atoms which are ionized outside the LCFS [13] as well in particular for those atoms which are ionized so close to the limiter surface that there gyration as W^+ ion intersects the surface (so-called prompt redeposition [15]). Both probabilities increase with decreasing ionization distance from the surface, which can be written (assuming constant plasma density) as

$$l_i = v/n_e\langle\sigma v\rangle = (2E)^{0.5}/m^{0.5}n_e\langle\sigma v\rangle$$

with v the velocity of the emitted tungsten, given by the energy (E) and mass (m) of the sputtered tungsten atoms, n_e the local plasma density and $\langle\sigma v\rangle$ the rate coefficient for ionization. By comparing physically sputtered carbon and tungsten atoms, l_i is about 10 times smaller for tungsten since the energy distribution is similar (determined by the surface binding energy U_s [14] and a cut-off energy of the energy distribution at higher energies) and $\langle\sigma v\rangle$ is larger for tungsten (about a factor 2–3 in the energy range of interest). At the highest local plasma densities obtained in TEXTOR ($\approx 1.2 \times 10^{13}/\mathrm{cm}^3$) measured tungsten ionization lengths are about 2 mm [7]. Prompt redeposition becomes important when the Larmor radius r_1 is comparable with the ionization length l_i. The ratio r_1/s is proportional to mn_e/B with B the magnetic field and to the ratio of the ionization rates, and is thus about a factor of 45 larger for tungsten than

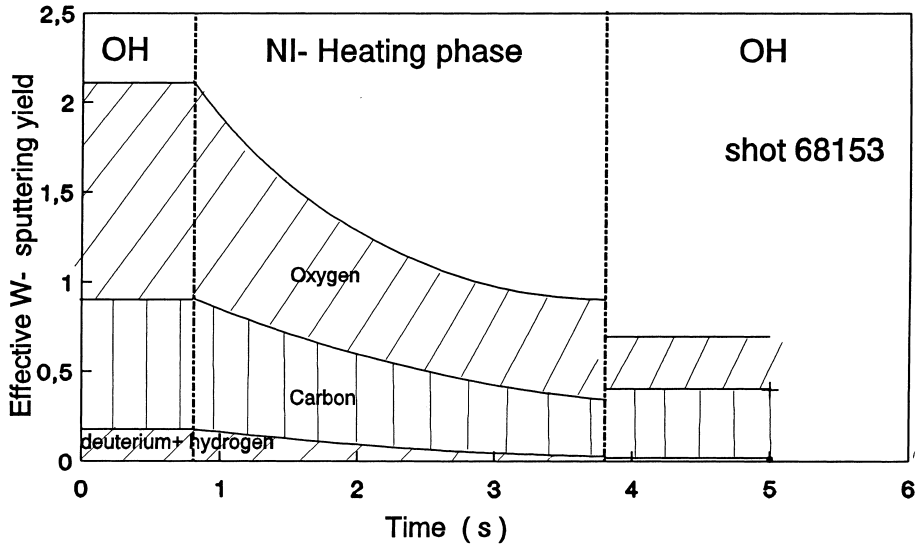

Fig. 4. Calculated amount of W-sputtering by hydrogen, deuterium, carbon and oxygen impact for the discharge shown in Fig. 2. A mixture of 50:50 H/D is used, a charge state of $Z = 4$ for carbon and oxygen and literature data on sputtering applied for maxwellian energy distribution shifted by the sheath potential.

for carbon, but is independent on the particle velocity and, on a first view, similar for sputtered and sublimed tungsten.

The redeposition of tungsten for the full testlimiter geometry has been calculated in detail with a local Monte Carlo Code ([16] ERO-TEXTOR). Tungsten is sputtered by deuterium, 2% carbon and 1% oxygen with charge states of 4 and 5, respectively, and emitted with a Thompson energy and cosine angular distribution. Tungsten atoms are followed until they are redeposited or leave the calculation volume which is 30 cm in toroidal 15 cm in poloidal and 5 cm in radial direction. A plasma temperatures of 80 eV and a density of 9×10^{12}/cm^3 is used which decreases along the magnetic flux surface to half of its value when approaching the limiter surface. More details can be found in Ref. [16]. The total sputter rate is about 2.3×10^{18} W-atoms/s and the fraction of total redeposition is about 55% of which about 80% are redeposited within the first gyration. The mean charge state of all redeposited tungsten is 1.5 and 1.1 for that part being promptly redeposited. The contribution of self-sputtering to the total tungsten release is about 13%. Zones of maximum particle fluxes, W-gross and net-erosion are positioned about 2–3 cm away from the tangency point. The calculations show a redeposition dominated area in the vicinity of the tangency point. This originates from tungsten sputtered at the strike zones which is then transported to top of the limiter.

3.3. Carbon and deuterium codeposition

CII carbon lines in front of the tungsten limiter result partly from directly reflected carbon, and partly from carbon which is implanted in the near surface layer and subsequently sputtered away by particle impact. On areas of net erosion the sticking of carbon and subsequent re-sputtering should result in a certain relative carbon to tungsten surface composition in the near surface region. In a rough estimation, the relative carbon surface concentration c_S is given by

$$F_c(1-R) = c_S[\Sigma F_i * Y_{ic}], \quad c_S = (1-R)/[\Sigma F_i/F_c * Y_{ic}]$$

with F_c and F_i the flux densities of carbon and other ion species, Y_{ic} the sputter yields of carbon on the W-surface by the impact of the different ion species, R is the particle reflection coefficient. For the conditions shown in Fig. 2 (2% C and O, physical sputtering of C only) c_S is calculated to be about 0.3 and does not change much with increasing density, since the decreased sputter rate of carbon with increasing density, leading to an increase of c_S, is compensated roughly by the simultaneously increasing carbon reflection coefficient R.

A W-limiter has been used for about 50 discharges at a radius of $r = 45$ cm under high densities of around 5×10^{13}/cm^3 and NBI-co + ICRH auxiliary heating varying between 1 and 3 MW. The limiter was preheated to about 750 K and the plasma impact raised the surface temperature routinely up to the range of 1500–2000 K at the end of the heating phase depending on the heating efficiency. Fig. 5 shows the limiter after the campaign. A shiny metallic area is visible ranging from the tangency point down to the side, which then changes to a black carbon-like appearance with a very sharp transition. Interference fringe analysis shows a steep increase of the layer thickness from zero up to about 300 nm on the ion drift side and to about 200 nm on the electron drift side. The steep increase occurs within about 4 mm.

Nuclear reaction analysis has been applied to detect the amount of deuterium and carbon, whereas hydrogen representing about 50% of the hydrogenic species could not been determined. No carbon nor deuterium was detectable on the shining areas (detection limit about 10^{15} C, D/cm^2) (Fig. 6). The figure shows a very sharp increase of the amount of deposited carbon, raising from zero up to about 10^{18}/cm^2 within about 3–4 mm on both sides. The layer is thicker on the ion drift side compared to the electron side which is consistent with the observed asymmetry of particles fluxes due to toroidal plasma rotation. These data are in excellent agreement with those from calorimetry. The deuterium content is also shown and corresponds to a D/C ratio of about 0.05–0.1 (the overall hydrogenic content can be higher due to the incorporation of hydrogen, which has not been measured). The low D/C ratio is the result of the high operational temperature of the limiter, which was above 700 K.

The figures show two surprising results: first, no carbon concentration could be measured on the shiny area (detection limit $\approx 2 \times 10^{15}$ C/cm^2). This indicates either a long range transport of carbon deep in the material, such that the carbon concentration is diluted below the detection limit or that the carbon has been evaporated from the surface due to excessive temperature excursions. Second, the transition from erosion to deposition areas is very sharp, with gradients of about 1000 nm/cm. This result can be understood taking into account the large differences in the reflection coefficient of carbon on carbon and carbon on tungsten. At some critical conditions the carbon concentration in the surface arises, which leads to even more carbon deposition due to a decreasing reflection, and finally, in a nonlinear habit, to the observed sharp boundary between both zones.

4. Summary

Tungsten, carbon and oxygen release has been measured by spectroscopy from tungsten limiters exposed beyond the radius of the ALT-II graphite belt limiter. Effective tungsten sputtering yields extend from about

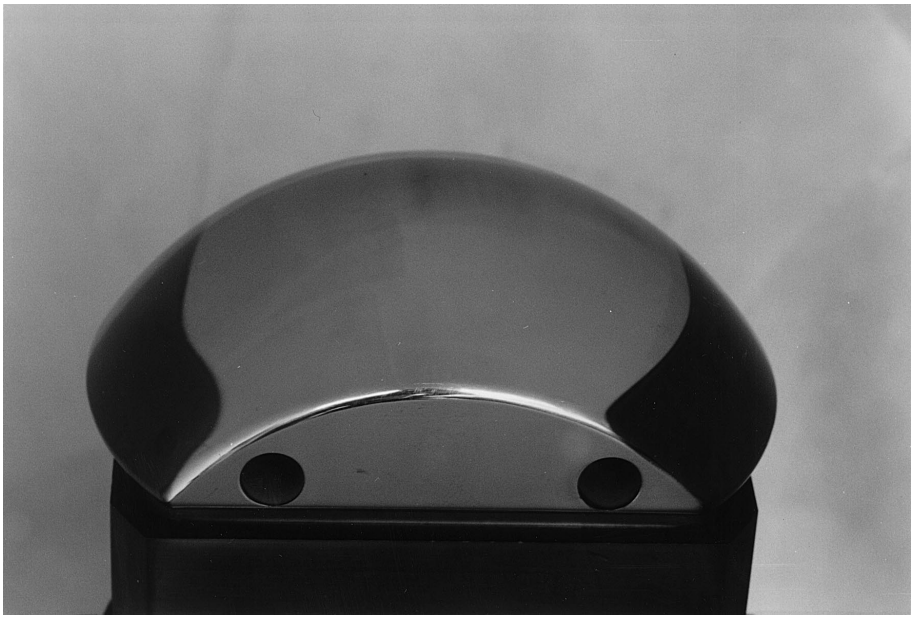

Fig. 5. Appearance of the W-limiter after use in about auxiliary heated 50 shots at $n_e = 4–5 \times 10^{13}/cm^3$ at $r = 45$ cm.

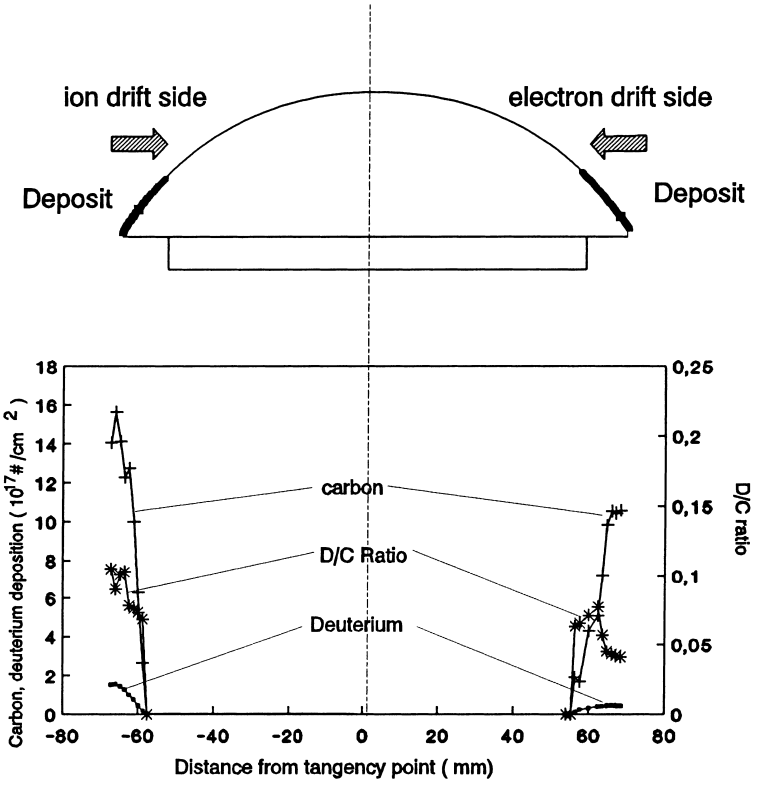

Fig. 6. Measured amount of deutrium and carbon (nuclear reaction analysis) across the midline of the limiter in torodial direction. The left side of the figure shows the D/C ratio.

3% at low plasma densities down to about 0.5% at the highest densities measured. Tungsten is nearly exclusively sputtered by carbon and oxygen and by a significant amount of self sputtering due to local redeposition. Model calculations based on measured deuterium, carbon and oxygen fluxes and sputter data show a good agreement with the effective tungsten release rate, but cannot fully explain the observed strong decrease of the W/H ratio with density.

Metallic shiny-like erosion zones are clearly separated from carbon deposit's. No carbon nor deuterium has been found by surface analysis in the shiny areas. A very sharp transition from the metallic surface to the carbon deposit occurs within about 2–4 mm. The carbon deposit is about 300 nm thick with a D/C ratio of 0.05–0.1. The sharp increase of the carbon deposition can be understood by the large difference in the carbon reflection coefficients on tungsten and on carbon, by which strong differences in the carbon deposition are possible on nearby areas.

References

[1] G. Frederici et al., ISNFT-4, Tokyo, 1997, to appear in Fusion Eng. Des.
[2] N. Noda, R. Neu, V. Philipps, J. Nucl. Mat. 241–243 (1997) 227.
[3] R. Neu, K. Asmussen, S. Deschka et al., J. Nucl. Mat. 241–243 (1997) 678.
[4] B. Lipschultz, J. Goetz, LaBombard et al., J. Nucl. Mat. 220–222 (1995) 967.
[5] V. Philipps, T. Tanabe, Y. Ueda et al., Nucl. Fusion 34 (11) (1994) 1417.
[6] Y. Ueda, T. Tanabe, V. Philipps et al., J. Nucl. Mat. 220–222 (1995) 240.
[7] M. Wada, V. Philipps, A. Pospeisczcyk, J. Nucl. Mat. 241–243 (1997) 799.
[8] J. Rapp, M.Z. Tokar, L. Könen et al., to be published in Plasma Physics and Contr. Fusion.
[9] M.Z. Tokar et al., Plasma Physics and Contr. Fusion 37 A241.
[10] A. Pospiesczcyk, Diagnostics of edge plasmas by optical methods, in: R.K. Janev, H.W. Drawin (Eds.), Atomic and Plasma Material Interaction Processes in Controlled Thermonuclear Fusion, Elsevier, Amsterdam, p. 213.
[11] K. Krieger, J. Roth, H. Annen et al., J. Nucl. Mat. 241–243 (1997) 684.
[12] M.Z. Tokar, Physica Scripta 51 665.
[13] B. Unterberg, H. Knauf, B. Lindner et al., J. Nucl. Mat. 241–243 (1997) 793.
[14] M.W. Thompson, Philos. Mag. 18 (1968) 377.
[15] D. Naujoks, K. Asmussen, M. Bessenrodt-Weberpals et al., Nucl. Fusion 36 (6) (1996) 671.
[16] U. Kögler, F. Weschenfelder, J. Winter et al., J. Nucl. Mat. 241–243 (1997) 816.